

ARTICLE

Growth modeling of the green microalga *Scenedesmus obliquus* in a hybrid photobioreactor as a practical tool to understand both physical and biochemical phenomena in play during algae cultivation

Deise P. Tramontin¹  | Pablo D. Gressler² | Leonardo R. Rörig² |
Roberto B. Derner³ | Jurandir Pereira-Filho⁴ | Claudemir M. Radetski⁵ |
Marinho B. Quadri¹

¹ Laboratório de Sistemas Porosos, UFSC, Universidade Federal de Santa Catarina, Florianópolis, Santa Catarina, Brazil

² Laboratório de Ficologia, UFSC, Universidade Federal de Santa Catarina, Florianópolis, Santa Catarina, Brazil

³ Laboratório de Cultivo de Algas, UFSC, Universidade Federal de Santa Catarina, Florianópolis, Santa Catarina, Brazil

⁴ Laboratório de Oceanografia Química, UNIVALI, Universidade do Vale do Itajaí, Itajaí, Santa Catarina, Brazil

⁵ Laboratório de Remediação Ambiental, UNIVALI, Universidade do Vale do Itajaí, Itajaí, Santa Catarina, Brazil

Correspondence

Deise P. Tramontin, Laboratório de Sistemas Porosos, UFSC, Universidade Federal de Santa Catarina—UFSC, Campus Trindade, Florianópolis, SC 88040-900, Brazil
Email: deiseparol@gmail.com

Funding information

Programa de Pós-Graduação em Engenharia Química (POSENQ - UFSC); Programa de Pós-Graduação em Biotecnologia e Biociências (PPGBB - UFSC); Conselho Nacional de Desenvolvimento Científico e Tecnológico; CAPES - Coordenação de Aperfeiçoamento de Pessoal de Nível Superior

Abstract

In recent years, numerous studies have justified the use of microalgae as a sustainable alternative for the generation of different types of fuels, food supplementation, and cosmetics, as well as bioremediation processes. To improve the cost/benefit ratio of microalgae mass production, many culture systems have been built and upgraded. Mathematical modeling the growth of different species in different systems has become an efficient and practical tool to understand both physical and biochemical phenomena in play during algae cultivation. In addition, growth modeling can guide design changes that lead to process optimization. In the present work, growth of the green microalga *Scenedesmus obliquus* was modeled in a hybrid photobioreactor that combines the characteristics of tubular photobioreactors (TPB) with thin-layer cascades (TLC). The system showed productivity greater than $8.0 \text{ g m}^{-2} \text{ day}^{-1}$ (dry mass) for CO_2 -fed cultures, and the model proved to be an accurate representation of experimental data with R^2 greater than 0.7 for all cases under variable conditions of temperature and irradiance to determine subsystem efficiency. Growth modeling also allowed growth prediction relative to the operating conditions of TLC, making it useful for estimating the system given other irradiance and temperature conditions, as well as other microalgae species.

KEYWORDS

hybrid photobioreactor, mathematical modeling, microalgae culture system, thin-layer cascade, tubular photobioreactor

1 | INTRODUCTION

Microalgae are predominantly photosynthetic organisms that use solar energy to combine water, carbon dioxide, and inorganic nutrients to

produce biomass rich in polysaccharides, proteins, lipids, and a range of secondary metabolites. Currently, the main uses of microalgal biomass involve food and feed products, but it is also a source for cosmetics, pharmaceuticals, pigments, fluorescent markers, antioxidants, and

vitamins (Hariskos & Posten, 2014). Much research has also focused on the potential use of microalgal biomass for the production of biofuels, either as biodiesel (from the transesterification of lipids), as biomass for fermentation and biogas production, or for the production of bioethanol and biohydrogen (Chisti, 2013; Kose & Oncel, 2017). In addition, microalgae cultivation can be used in bioremediation processes, encompassing assimilation of nutrients, CO₂, metals, and organic pollutants (Henkanatte-Gedera et al., 2015; Kang & Wen, 2015; Kumar, Dahms, Won, Lee, & Shin, 2015).

The high genetic diversity of this multiphyletic group of organisms results in an equivalent diversity of chemical composition, which can be modified through genetic manipulation or by variations in ambient and stress conditions, as well as harvesting at different periods of the growth cycle (Guihéneuf, Khan, & Tran, 2016; Minhas, Hodgson, Barrow, & Adholeya, 2016; Spolaore, Joannis-Cassan, Duran, & Isambert, 2006).

The adjustment of culture conditions to optimize growth and obtain products of interest begins at laboratory scale with bench tests to understand the physiological responses and environmental requirements for each strain. Subsequently, such adjustments need to be extrapolated to larger scales in order to be effective as a viable productive process. It is in this scale up transition that many challenges lie. Consequently, experimentation with replication is required, as well as engineering advancements and the innovation necessary to provide maximal growth at the lowest cost.

Many different microalgae cultivation systems (MCS), or photo-bioreactors, have been developed to optimize the supply of light, CO₂, and nutrients with minimum energy and input costs. The main classification of culture systems takes into account the degree of exposure of the culture to environmental conditions. Thus, we see open systems that take advantage of sunlight at the expense of control over environmental conditions, closed systems with a greater degree of control over environmental conditions, and hybrid systems that combine elements of both open and closed systems (Öncel & Akpolat, 2006).

Open systems are the oldest and most widely used configurations for mass production of microalgae (Borowitzka, 1999; Pulz, 2001). They may be shallow rectangular tanks, such as those used for the cultivation of *Dunaliella salina* microalgae; circular with a mixer arm, widely used for cultivation of *Chlorella* spp., or long canals in a single or multiple circuit configuration and agitated by paddle wheels. These are known as paddle wheel mixed raceway ponds, or raceway ponds, but now called raceways (Chisti, 2016), and they are widely used for cultivation of *Arthrospira* spp. Thin-layer cascades (TLC) are perhaps the open systems that have been most improved in the last decades. In this type of system, turbulence is created by gravity such that the suspension culture flows on a ramp. This allows the culture to be grown in very thin layers (averaging 1.0–5.0 cm in height), optimizing the use of light owing to its high surface-to-volume (S/V) ratio (Masojídek & Prasil, 2010; Morales-Amaral, Gómez Serrano, Acién, Fernández-Sevilla, & Molina Grima, 2015).

The main closed MCS are flat panel, tubular (horizontal, inclined, or vertical), bubble column, airlift, and stirred tank reactors

(Xu, Weathers, Xiong, & Liu, 2009). In addition to greater control over environmental conditions, closed MCS suffer less from contamination, allowing efficient gas exchange and better light utilization, but they are more expensive to construct and maintain (Pulz & Scheibebogen, 1998).

Since the 1980s, several researchers have suggested combining open and closed systems, trying to take advantage of each type of bioreactor. In this sense, systems were proposed combining raceways with tubular PBRs, as well as other configurations, some of which operated on a pilot scale (Pushparaj, Pelosi, Tredici, Pinzani, & Materassi, 1997).

The mathematical modeling of growth processes adjusted for the specific configuration of each MCS is very useful for understanding, describing, and scaling up these systems. It allows response prediction and design guidance, thus enabling efficient operation and control, in addition to simulating biomass production processes more quickly and accurately, orienting corrections, readjustments, and improvements for optimization (Bernard, Mairet, & Chachuat, 2015). It is, therefore, a way of organizing disconnected information from experimental data in an organized way, pinpointing interactions relevant to the system, and understanding behavior and characteristics that are qualitatively important to the process. In this way, the development of realistic models for microalgae culture involves coupling separate submodels (Bernard et al., 2015). For example, one may include intrinsic biological properties, such as growth, decay, and biosynthesis, as well as the effects of light and temperature on these processes, while another considers the effects of physical properties, such as hydrodynamics, light attenuation, and temperature on the culture. In addition, it is necessary to perform tests of the different existing models linked to certain answers and also the application of models thought for a certain purpose from other perspectives. An example of this is what Ritchie (2008) did by testing different types of models (Michaelis-Menten, Waiting in Line Model, exponential saturation, hyperbolic tangent) for the variation of photosynthesis as a function of light.

Some available models require the input of many parameters, thus imposing limitations on their use (Huesemann et al., 2013; Quinn, Winter, & Bradley, 2011). The predictability of these models for different species is questionable since they need validation in addition to their complexity, and some parameters can be difficult to estimate (Béchet, Shilton, & Guieysse, 2013; Lee, Jalalizadeh, & Zhang, 2015).

Also, models using independent variables for irradiance and temperature do not take into account the interdependence of these conditions in relation to the rate of photosynthesis. That is, they are solved separately, generating only one representative value.

Despite this drawback, mathematical modeling is still the most recommended approach owing to the reduction of overfitting risks (Béchet et al., 2013; Bernard & Rémond, 2012). In this context, we include the exploration of macromodels that can cover a series of parameters simultaneously and, hence, approximate the mathematical modeling of the open systems (Fernández, Camacho, Pérez, Sevilla, & Grima, 1998; Guterman, Vonshak, & Ben-Yaakov, 1990).

In the present study, the growth of the green microalga *Scenedesmus obliquus* (Turpin) Kützing was evaluated in a hybrid MCS that combines the characteristics of TLC and TPB. A mathematical model was developed using a system of independent variables, allowing us to estimate how changing physical parameters, such as width, length, thin-layer thickness dimensions, and environmental parameters, such as temperature, irradiance, and CO₂ concentration, for a given microalgae species will affect the system's efficiency, which, in turn, will lead to clues about how each variable behaves in the growth process.

2 | MATERIALS AND METHODS

2.1 | Culture system

We used an algal culture system that fits the description of a hybrid MCS, combining the working principles of the thin layer cascade (TLC) and the tubular photobioreactor (TPB). The TLC favors gas exchange and temperature maintenance, and it provides a larger area of exposure to sunlight (Doucha & Lívanský, 2006; Lívanský & Doucha, 1996; Masojádek, Kopecký, Giannelli, & Torzillo, 2010). The TPB optimizes the use of injected CO₂, as a result of the greater contact of gas with the culture over time (Grima, Fernández, Ación, & Chisti, 2001; Sevilla et al., 2004). The system operates continuously, and both TLC and TPB work together. The culture from the TLC section flows to a reservoir where it is pumped into two transparent acrylic tubes, 10 cm in diameter and 2 m high (15.7 L each), before reaching the TLC section again. The tubes were incorporated into the system in order to

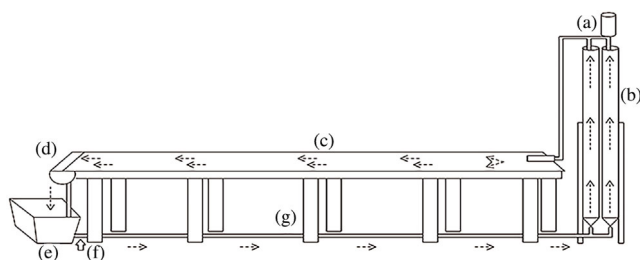


FIGURE 1 [above] Schematic illustration of the hybrid culture system. Arrows indicate the flow direction. Identification of the main components from left to right: (a) auxiliary degasser, (b) pipes, (c) ramp, (d) gutter, (e) reservoir with pump, (f) CO₂ injection, (g) connection of the reservoir to the pipes. [below] Photograph of the system in operation. See text and Table 1 for dimensions and details

prolong contact time between culture and CO₂ that is supplied at the outlet of the reservoir (Figure 1).

Two 1/6 HP submersed pumps operate in parallel. For calculation purposes, the volume of the tubes (TPB) was included in the volume of the reservoir. Table 1 presents the dimensions and operating conditions of the system.

Losses by evaporation were restored by continuous supply of water controlled by a ballcock valve installed in the reservoir. The water provided had physicochemical characteristics (pH and temperature) similar to those of the circulating medium in the system, but without addition of nutrients and without chlorine. A clear acrylic cover was built to prevent dilution of the medium by rain. The design is an adaptation of the traditional TLC systems and is being submitted to patenting in the National Institute of Intellectual Production (INPI, Brazil).

2.2 | Microalgae and culture conditions

The tests were carried out using a strain of *S. obliquus* (Turpin) Kützing obtained from the Laboratory of Algal Culture (LCA-UFSC). Cultures were inoculated into the system containing, on average, 3×10^6 cells ml⁻¹. Culture medium was used, as proposed by Provasoli (1968) and as modified by LCA-UFSC, and it was composed of 1.05 g L⁻¹ NaNO₃, 1.25 g L⁻¹ MgSO₄ · 7H₂O, 0.658 g L⁻¹ NaH₂PO₄, 0.02 g L⁻¹ FeCl₃ · 6H₂O, and 1.0 g L⁻¹ NaHCO₃. Four experimental batch cycles lasting 126 hr without nutrient replacement were evaluated. Batches 1 and 2 did not receive CO₂. Batches 3 and 4 received intermittent injection of CO₂, from 6:00 AM to 7:00 PM, representing daylight hours in the region for the season. The injection regimen consisted of supply for 15 min, with flow rate of 1 ml min⁻¹, and suspension for 30 min.

TABLE 1 Dimensions and operating conditions of the culture system

Features of the system	
Flow rate	55.7 L min ⁻¹
Flow speed	2.965 m s ⁻¹
Total operational volume of culture	163 L
Maximum volume of culture in the system	180 L
TLC section	
Length of the ramp	5.0 m
Width of the ramp	1.0 m
Liquid column thickness	0.01 m
Operational volume of culture in the section	50 L
TPB section	
Length of the tubes	2.0 m
Internal width of the tubes	0.01 m
Operational volume of culture in the tubes	31.4 L
Reservoir	
Operational volume of culture	81.6 L

2.3 | Biomass measurement

Samples for biomass measurement of were collected daily with a smaller time interval in the first 3 days of cultivation to follow the exponential growth phase. Dry algal biomass (g L^{-1}) was determined by gravimetry, according to Vega and Voltolina (2007). Known culture volumes were filtered through glass-fiber filters (GF-F, $0.22 \mu\text{m}$, 47 mm diameter) pre-calcined at 490°C for 20 min, kept for 1 hr in a desiccator, and weighed in an analytical balance (precision 0.0001 g). After filtration, filters were oven dried at 105°C for 12 hr, kept for 1 hr in a desiccator, and again weighed. The weight difference obtained refers to the dry algal biomass.

2.4 | Phosphorus consumption

Phosphorus is used in cellular processes for energy transfer and nucleic acid synthesis, and it is preferably taken from inorganic phosphates dissolved in H_2PO_4 and HPO_2 forms. The rate of P consumption depends on the concentration of P in the medium, intracellular P content, pH, ion concentrations, such as Na^+ , K^+ , and Mg^{2+} , and temperature (Kaplan, Pratt, & Pedersen, 1986). In the present study, the total dissolved phosphorus (TDP) concentration was determined during the growing time to evaluate its consumption and was used as an indirect tracer of microalgae growth and productivity. The 4500 P colorimetric method of the Standard Methods for the Examination of Water and Wastewater (APHA, 2012) was used. The samples were filtered through glass fiber filters (GF-F, $0.22 \mu\text{m}$, and 47 mm in diameter). In cases of excess biomass, the samples were previously centrifuged.

2.5 | Physical and physicochemical parameters

Temperature and irradiance, physical factors directly influencing algal physiology, were continuously recorded throughout the experimental period through a HOBO® Pendant Data Logger model UA-002-64 immersed in the central region of the ramp. Data were processed using the HOBO® Ware Pro software, version 3. Dissolved oxygen saturation (%DO) and pH were measured at the end of the ramp by YSI 5000 Oximeter and Thermo Scientific Orion Star AZ11 pH meter, respectively.

2.6 | Determination of optimal light intensity (I_{opt}) for microalgae growth

The optimal light intensity (I_{opt}) for a microalgae culture is a specific parameter for each strain, and such data are necessary for the mathematical modeling of growth. This parameter is determined experimentally. For the strain used in this study, an adaptation of the technique, termed "light-gradient box incubation," was used (Forget et al., 2007). A series of exponentially growing culture flasks was exposed to a light gradient, and photosynthetic production was assessed through the response in oxygen production in each flask over time. A light source emitting irradiance of $2,100 \mu\text{mol m}^{-2} \text{ s}^{-1}$ was installed at the end of a closed chamber without influence of external light. The first flask received maximum irradiance, and the remaining flasks received progressively smaller irradiances as a function of the shading of the

previous flasks. The irradiance received in each flask within the chamber was measured with a LI-1400 radiometer equipped with a calibrated underwater quantum sensor LI-190SA (both from LI-COR, Inc., Lincoln, NE). Temperature within the chamber was maintained constant through continuous flow of water during experimental development. The flasks were filled with modified C medium (Provasoli, 1968) and culture containing $1.5 \times 10^6 \text{ cells ml}^{-1}$. The last flask was covered with foil so that it was totally without light (dark flask). This flask was used to estimate the respiration of the culture. The initial and final concentrations of dissolved oxygen were measured in each flask with a YSI 5000 oximeter equipped with a 5010 OD sensor (YSI, Inc., Yellow Springs, OH). Exposure times were 45, 90, 135, and 180 min.

The initial chlorophyll-*a* concentration in the algal culture was determined for purposes of relativization of primary productivity. The fluorometric method was used according to Arar and Collins (1997). Chlorophyll-*a* concentration was determined with a calibrated Turner Trilogy® fluorometer with optical kits 7200-046.

Gross primary productivity was determined according to Equation 1. A photosynthetic quotient of 1.2 and a respiratory coefficient of 0.8 were used to convert produced and consumed dissolved oxygen values, respectively, into consumed and produced CO_2 (Macedo, Ferreira, & Duarte, 1998).

$$\text{GPP} = \frac{1.2 \times (\text{DO}_{\text{Lf}} - \text{DO}_{\text{Li}}) + 0.8 \times (\text{DO}_{\text{Di}} - \text{DO}_{\text{Df}})}{(\text{Chl} - a \times t_{\text{exp}})} \quad (1)$$

where GPP is gross primary production ($\text{mg C mg Chl-}a^{-1} \text{ hr}^{-1}$); DO_{Li} is initial dissolved oxygen in the flask exposed to light ($\text{mg O}_2 \text{ L}^{-1}$); DO_{Lf} is final dissolved oxygen in the flask exposed to light ($\text{mg O}_2 \text{ L}^{-1}$); DO_{Di} is initial dissolved oxygen in the dark flask ($\text{mg O}_2 \text{ L}^{-1}$); DO_{Df} is final dissolved oxygen in the dark flask ($\text{mg O}_2 \text{ L}^{-1}$); *Chl-a* is Chlorophyll-*a* concentration ($\text{mg Chl-}a \text{ L}^{-1}$) and t_{exp} is light exposure time (hr).

I_{opt} was obtained from the plot of GPP as a function of irradiance (*P* vs. *I* curve), being the value of *I* that generated maximum GPP in each experiment (maximum production, P_{max}).

2.7 | Mathematical modeling

Submodels for nutrient consumption, irradiance, and temperature came from the literature. For nutrient consumption, the Monod model was used. It is a simple model based only on nutrient consumption to estimate growth, and it does not take into account irradiance and temperature. The irradiance model determines the influence of photosynthesis on growth. Similar to the temperature model, which uses variable dynamics, parameters of experimental origin are related to parameters associated with the given species. The Monod model is the basis for the description of the intervening parameters in growth kinetics. It is an unstructured model and one of the most used to represent growth of microorganisms (Hiss, 2001). Equation 2 presents the Monod model.

$$\mu = \mu_m \left(\frac{S}{k_s + S} \right) \quad (2)$$

where S is substrate concentration (g L^{-1}); μ is specific growth rate (hr^{-1}); μ_m is maximum specific growth rate (hr^{-1}); and k_s is substrate half saturation constant (g L^{-1}).

The growth rate can be related to the rate of substrate (phosphorus) consumption through the cell yield coefficient ($Y_{X/S}$). This relationship is presented in Equation 3 and was applied to phosphorus and CO_2 consumption (Hiss, 2001).

$$\frac{dS}{dT} = -\frac{1}{Y_{X/S}} \cdot \frac{dX}{dT} \quad (3)$$

where $Y_{X/S}$ is cell biomass formed by mass of substrate consumed (g g^{-1} ; see Equation 4).

$$Y_{X/S} = \frac{X_f - X_0}{S_0 - S_f} \quad (4)$$

where X_f is final biomass concentration (g L^{-1}); X_0 is initial biomass concentration (g L^{-1}); S_0 is initial substrate concentration (g L^{-1}); and S_f is final substrate concentration (g L^{-1}).

The irradiance model is based on the equation of Steele (1962). It is a variation of the model presented by Di Toro, O'Connor, and Thomann (1971), and it generates a dimensionless factor between 0 and 1, with 1 as the optimal value. The parameters of this model can be defined externally or environmentally, which is uncontrollable, as in the case of incident irradiance, or internally or physiologically, as in the present case in reference to the algae used. Equation 5 describes the model used.

$$f(I) = \frac{I}{I_{\text{opt}}} \text{Exp}\left(1 - \frac{I}{I_{\text{opt}}}\right) \quad (5)$$

where I is incident irradiance ($\mu\text{mol m}^{-2} \text{s}^{-1}$) and I_{opt} is optimum irradiance ($\mu\text{mol m}^{-2} \text{s}^{-1}$).

The I_{opt} value used was the mean of the I_{opt} values obtained from the four P versus I curves. I values are experimental in origin, being a function generated over time. For simplification, the integral of this curve was made considering the integration interval of 1 hr. This model does not rely on parameters relative to self-shading because the experimental unit has a thin layer of culture that flows in a turbulent way; therefore, this phenomenon was discounted.

The Cardinal Temperature Model, as initially proposed by Lobry, Rosso, and Flandrois (1991), was used to evaluate the influence of this variable on the system. This model includes four parameters, three of which have physiological significance in this case by their relationship to the algae used, which is capable of presenting growth rates between T_{min} and T_{max} . The model is described by Equation 6.

where T_{min} is temperature below which no growth is observed [$^{\circ}\text{C}$]; T_{max} is temperature above which no growth is observed [$^{\circ}\text{C}$]; T_{opt} is temperature at which maximum specific growth occurs [$^{\circ}\text{C}$]; and T is temperature of the system [$^{\circ}\text{C}$]. The values of T_{min} , T_{max} , and T_{opt} for *S. obliquus* were obtained from Hodaifa, Martínez, and Sánchez (2010). For T values, the experimental data were used and were inserted in the form of an integrated function over time.

2.8 | Aspects of mass transfer

Aspects of mass transfer were considered in the system's balance. For simplification, when CO_2 was injected, the system was considered saturated throughout the experimental period.

The fraction of CO_2 in equilibrium with the liquid medium was calculated using Henry's law, according to Equation 7.

$$x_2 \times H = y_2 \times P \quad (7)$$

where x_2 is a fraction of CO_2 in equilibrium with the liquid medium; H is Henry's constant [MPa]; y_2 is the fraction of CO_2 in equilibrium with the air; and P is total pressure of the system [MPa].

The convective mass transfer coefficient was calculated according to Welty, Wicks, Wilson, and Rorrer (2008) by the penetration theory according to Equation 8.

$$k_L = \sqrt{\frac{D_{AB} \times v_{\text{ave}}}{\pi \times C_{\text{ls}}}} \quad (8)$$

where k_L is convective coefficient of mass transfer [m s^{-1}]; D_{AB} is mass diffusion coefficient of solute A in solvent B [$\text{m}^2 \text{s}^{-1}$]; v_{ave} is average flow velocity [m s^{-1}]; and C_{ls} is length of liquid surface [m]. The diffusion coefficient was estimated by the correlation proposed by Wilke and Chang (1955) for diluted non-electrolyte solutes.

2.9 | Elaboration of differential balances

Differential balances were determined separately for TLC and TPB. The volume of TPB was considered to be the sum of the volume of the tubes and the reservoir. For simplification, four assumptions were made. First, it was assumed that the reservoir was perfectly stirred, that is, as soon as the flow enters the reservoir, the same concentration of volume inside of it was assumed to be equal to the output concentration. Second, the concentration in the TLC section was treated as the arithmetic mean between the input and output values. Third, β was an adjustment variable to determine the efficiency of the TPB section in relation to the TLC section. Fourth, for cellular balance, the generation term was calculated as a function of the minimum value of phosphorus and CO_2 calculated by the Monod model in addition to the reduction factors related to Irradiance [$f(I)$] and temperature [$f(T)$],

$$f(T) = \left(\frac{(T - T_{\text{max}}) \times (T - T_{\text{min}})^2}{(T_{\text{opt}} - T_{\text{min}}) \times [(T_{\text{opt}} - T_{\text{min}}) \times (T - T_{\text{opt}}) - (T_{\text{opt}} - T_{\text{max}}) \times (T_{\text{opt}} + T_{\text{min}} - 2 \times T)]} \right) \quad (6)$$

according to equation 9. Mass transfer was considered to occur only in the TLC section since it presents greater turbulence and greater surface availability for gas exchange. The model is a system of differential equations in relation to the time that they are solved in coupled form. Equations 9 to 14 represent the proposed differential balances.

$$\frac{dXe}{dt} - \beta \times \text{Min} \left[\left(\frac{\mu_{\max S} \times S}{k_s + S} \right), \left(\frac{\mu_{\max C} \times \text{CO}_2}{k_c + \text{CO}_2} \right) \right] \times f(I) \times f(T) \times Xe[t] \\ = - \frac{v_{\text{ave}} \times H_{\text{col}} \times L_{\text{col}}}{\text{Vol}} \times (X[t] - Xe[t]) \quad (9)$$

$$\frac{\left(\frac{dX}{dt} + \frac{dXe}{dt} \right)}{2} - \text{Min} \left[\left(\frac{\mu_{\max S} \times S}{k_s + S} \right), \left(\frac{\mu_{\max C} \times \text{CO}_2}{k_c + \text{CO}_2} \right) \right] \times f(I) \times f(T) \\ \times \left(\frac{X[t] + Xe[t]}{2} \right) = - \frac{v_{\text{ave}}}{C_{\text{col}}} \times (X[t] - Xe[t]) \quad (10)$$

$$\frac{dSe}{dt} + \frac{\left(\frac{\mu_{\max S} \times S}{k_s + S} \right) \times f(I) \times f(T)}{\left(\frac{X_F - X_0}{S_0 - S_F} \right)} \times Xe[t] = \frac{v_{\text{ave}} \times H_{\text{col}} \times L_{\text{col}}}{\text{Vol}} \times (S[t] - Se[t]) \quad (11)$$

$$\frac{\left(\frac{dS}{dt} + \frac{dSe}{dt} \right)}{2} + \frac{\left(\frac{\mu_{\max S} \times S}{k_s + S} \right) \times f(I) \times f(T)}{\left(\frac{X_F - X_0}{S_0 - S_F} \right)} \times \left(\frac{X[t] + Xe[t]}{2} \right) \\ = - \frac{v_{\text{ave}}}{C_{\text{col}}} \times (S[t] - Se[t]) \quad (12)$$

$$\frac{dCe}{dt} + \left(\frac{Ce[t]}{Xe[t]} \right) \times \left(\left(\frac{\mu_{\max C} \times Ce[t]}{k_c \times Ce[t]} \right) \times f(I) \times f(T) \right) \times Xe[t] \\ = \frac{H_{\text{col}} \times L_{\text{col}} \times v_{\text{ave}}}{\text{Vol}} \times (C[t] - Ce[t]) \quad (13)$$

$$\left(\frac{dC}{dt} + \frac{dCe}{dt} \right) - \left(k_L \times \frac{C_{\text{col}} \times L_{\text{col}}}{C_{\text{col}} \times L_{\text{col}} \times H_{\text{col}}} \times (C_{\text{CO}_2} - C[t]) \right) + \left(\frac{\left(\frac{C[t] + Ce[t]}{2} \right)}{\left(\frac{X[t] + Xe[t]}{2} \right)} \right) \times \left(\frac{Ce[t]}{Xe[t]} \right) \times \left(\left(\frac{\mu_{\max C} \times Ce[t]}{k_c \times Ce[t]} \right) \times f(I) \times f(T) \right) \times \left(\frac{X[t] + Xe[t]}{2} \right) = - \frac{v_{\text{ave}}}{C_{\text{col}}} \times (C[t] - Ce[t]) \quad (14)$$

where Xe is input biomass concentration at the TLC section [g L^{-1}]; X is output cell concentration at the TLC section [g L^{-1}]; Se is input phosphorus concentration at the TLC section [g L^{-1}]; S is output phosphorus concentration at the TLC section [g L^{-1}]; Ce is input CO_2 concentration at the TLC section [g L^{-1}]; C is output CO_2 concentration at the TLC section [g L^{-1}]; H_{col} is height of the liquid column at the TLC section [m]; L_{col} is width of the liquid column at the TLC section [m]; Vol is culture volume at the TPB section [L]; β is the adjustment parameter that determines the efficiency of the TLC section in relation to the TPB section, given its geometric and phenomenological differences, and t is time [hr]. The other variables have already been mentioned.

The initial conditions that provide solutions to these differential equations are as follows: $X[0] = Xe[0] = X_0$ = initial cell concentration; $S[0] = Se[0] = S_0$ = initial phosphorus concentration; $C[0] = Ce[0] = C_{\text{CO}_2}$ = Concentration of CO_2 in the liquid in equilibrium with the concentration of the component in the atmosphere.

2.10 | Loading of experimental data in the mathematical model

Following the elaboration of differential balances, the experimental data of temperature and irradiance were then loaded. Afterwards, the values of T_{\max} , T_{\min} , T_{opt} were derived from the studies of Hodaifa et al. (2010) for *S. obliquus* and I_{opt} from the P versus I curve. After defining these conditions, it was necessary to insert the initial and final concentrations of biomass and phosphorus and finally the culture time so that the model would be solved for this established range. Similarly, the model, as elaborated, was adapted to the experimental conditions of Masojidek et al. (2010) with respect to the form of substrate feeding in the environment, operating conditions of the system, environmental conditions of cultivation, and initial and final biomass and microorganism used.

2.11 | Determination of efficiency of TPB section

Before adjusting the model to experimental data, a study was performed to determine the efficiency of the TPB section because it is well known that each section has different features. Parameter β in Equation 9 is a correction value for the specific growth rate and is considered in the cell balance at the input of the TLC section, that is, output from the TPB section. This parameter compares the efficiency of one subsystem against the other because the TLC section is considered optimal, that is, equal to 1. The study consisted of varying the efficiency of parameter β from 0 to 1 for each situation and adjusting the kinetic constants to obtain a R^2 closer to 1 for each culture.

3 | RESULTS AND DISCUSSION

3.1 | Environmental conditions during the experimental assays

In the four cultivation experiments performed, the environmental variables temperature and irradiance showed typical values for the summer condition in this study subtropical region (Figure 2).

Primary productivity is directly influenced by temperature and irradiance, and its monitoring is fundamental throughout the growing period. During all four evaluated cultivations, temperature values showed significant oscillation accompanying irradiance variation between the day and night periods, reaching a thermic amplitude of 20°C in some cases. During almost all cultivation days, the climate was sunny, except for the initial hours of Batch 1 and half of the period of Batch 2 when cloudy days were recorded with eventual rainfall. Very high irradiances, which were recorded at

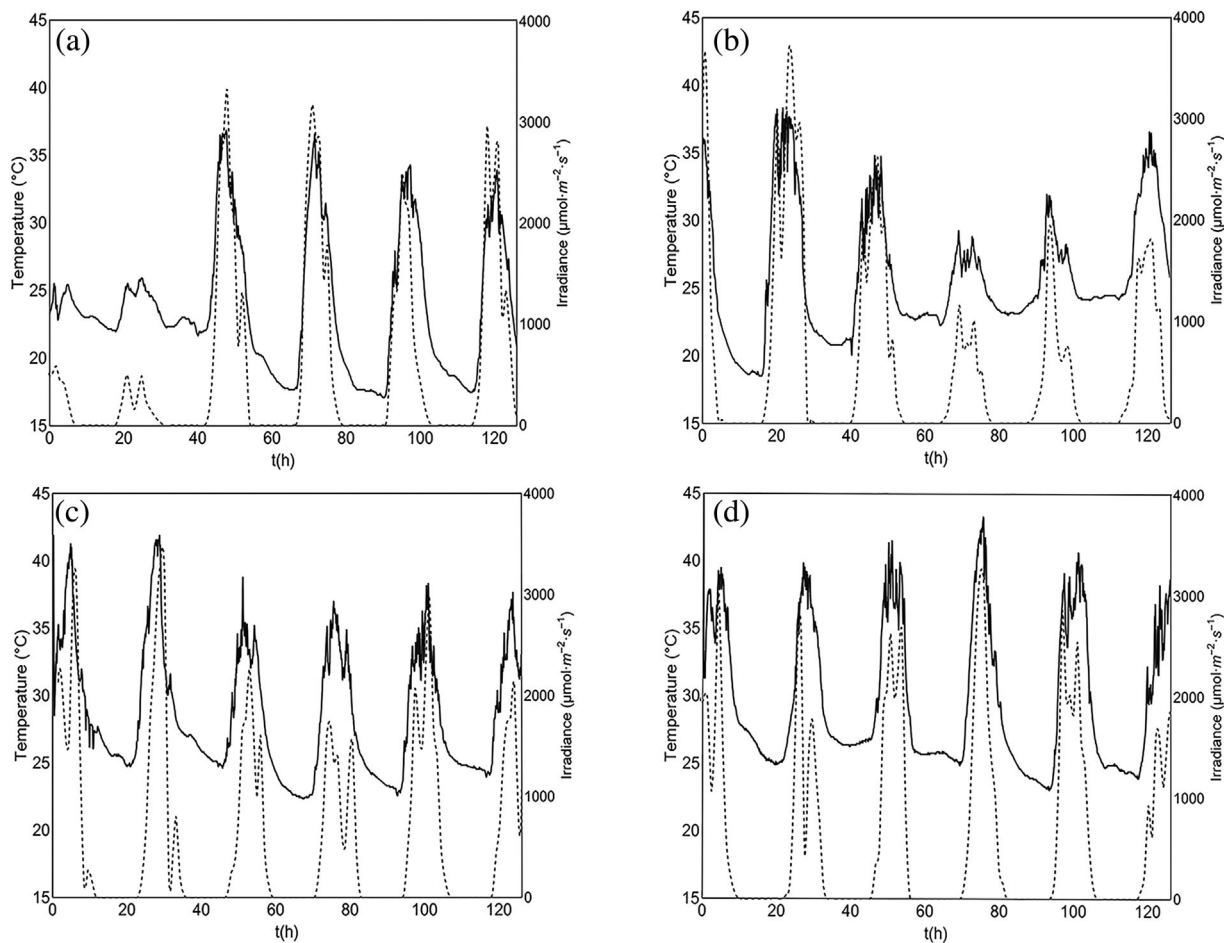


FIGURE 2 Water temperature (solid line) and integrated irradiance (dashed line) during the four experimental batches evaluated. (a) Batch 1, (b) Batch 2, (c) Batch 3, (d) Batch 4

various times in all experiments, may cause photoinhibition of algae, limiting the photosynthetic process and reducing primary productivity. In the present system, turbulence at high irradiance in the TLC section was followed by a less turbulent condition with lower irradiance in the reservoir and in the TPB section, which could have attenuated the effects of photoinhibition and photosaturation, despite the low residence time of the culture in this section. High temperatures and their daily oscillation could have reduced efficiency of the process, as well, since all species have their optimum growth within generally narrow bands, although they can be tolerant to higher temperatures, as well as temperature variations, during the growth cycle (Martínez, Jimenez, & Yousfi, 1999). On the other hand, higher temperatures accelerate the transfer of dissolved oxygen from the water to the air, which positively affects the photosynthetic process because produced oxygen is a limiting factor for photosynthesis (Shelp & Canvin, 1980). These temperature and irradiance oscillations were expected because the system was installed in an open place. Figure 3 shows the variations of pH and dissolved oxygen saturation (% DO). The pH values generally tended to increase during the day and decrease at night as a function of the algal photosynthesis cycle. In

the batches with CO₂ injection, lower values of pH were observed, especially in the batch 4. The % DO also showed oscillations throughout the batches, however, with values always higher than 100% in the batches without CO₂ injection, and periods with values lower than 100% when CO₂ was injected. Despite this apparent negative relation between CO₂ injection and % DO, probably the lower values of % DO in the CO₂ batches were related to the higher temperature values registered in these experiments (Figure 2).

3.2 | *P* versus *I* curve

P_{\max} and I_{opt} values obtained in the incubation experiment are presented in Figure 4. The highest productivity value was obtained with 90 min of incubation. For longer incubation times (135 and 180 min), productivity dropped, possibly indicating the saturation effect of photosynthesis or carbon limitation. However, none of the incubations showed photoinhibition on the *P* versus *I* curve. Greater tolerance to high irradiance is desirable in crops exposed to sunlight in tropical and subtropical regions (Gómez-Villa, Voltolina, Nieves, & Piná, 2005), especially considering the characteristics of the cultivation system used.

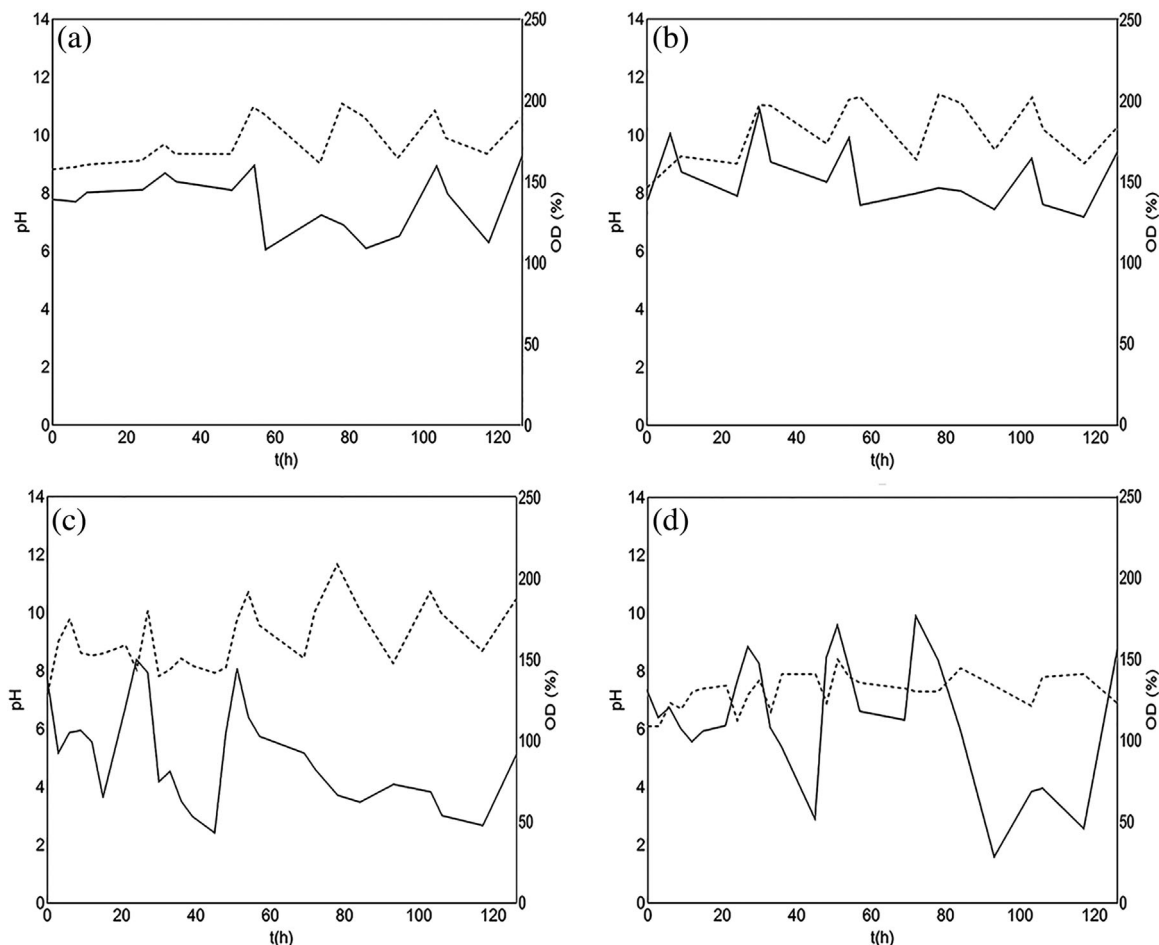


FIGURE 3 Dissolved oxygen saturation—OD (%) (solid line) and pH (dashed line) during the four experimental batches evaluated. (a) Batch 1, (b) Batch 2, (c) Batch 3, (d) Batch 4

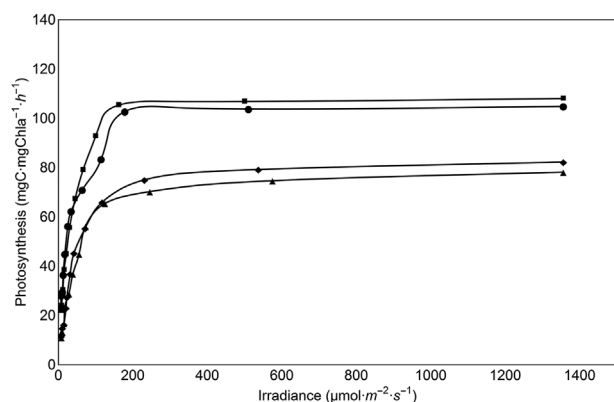


FIGURE 4 Photosynthesis per unit chlorophyll versus irradiance (P vs. I curve) in different incubation times. Solid circle: 45 min incubation ($P_{\max} = 100.72 \text{ mgC mg Chla}^{-1} \text{ hr}^{-1}$, $I_{\text{opt}} = 178.20 \mu\text{mol m}^{-2} \text{ s}^{-1}$), solid square: 90 min incubation ($P_{\max} = 105.32 \text{ mgC mg Chla}^{-1} \text{ hr}^{-1}$, $I_{\text{opt}} = 162.00 \mu\text{mol m}^{-2} \text{ s}^{-1}$), empty lozenge: 35 min incubation ($P_{\max} = 75.00 \text{ mgC mg Chla}^{-1} \text{ hr}^{-1}$, $I_{\text{opt}} = 230.80 \mu\text{mol m}^{-2} \text{ s}^{-1}$), empty triangle: 180 min incubation ($P_{\max} = 70.23 \text{ mgC mg Chla}^{-1} \text{ hr}^{-1}$, $I_{\text{opt}} = 245.50 \mu\text{mol m}^{-2} \text{ s}^{-1}$)

The mean value of I_{opt} obtained in the P versus I curves ($204.13 \mu\text{mol m}^{-2} \text{ s}^{-1}$) was adopted as reference in the irradiance model comprising the differential balances. This value was within the expected range, but it could always vary according to the incubation technique used, the source of illumination, the concentration of microorganisms and exposure time.

Gris, Morosinotto, Giacometti, Bertucco, and Sforza (2014) evaluated the influence of irradiance on *S. obliquus* cultivated with BG11 medium in a flat plate photobioreactor, and they obtained a maximum growth rate at $150 \mu\text{mol m}^{-2} \text{ s}^{-1}$. Ruiz Marín, Mendoza-Espinosa, and Stephenson (2010), in turn, grew immobilized *S. obliquus* and verified greater cellular growth and protein content at $200 \mu\text{mol m}^{-2} \text{ s}^{-1}$. Thus, the values obtained in the present study are within the range expected for the species.

3.3 | Efficiency of TPB section

It was previously explained that the purpose of the TLC section was to optimize the use of irradiance and also facilitate O_2 dissipation, while the TPB section is designed to optimize the mixture and use of CO_2 . However, when passing through the tubes and reservoir of the TPB section, the culture also receives light. Thus, despite lower exposure

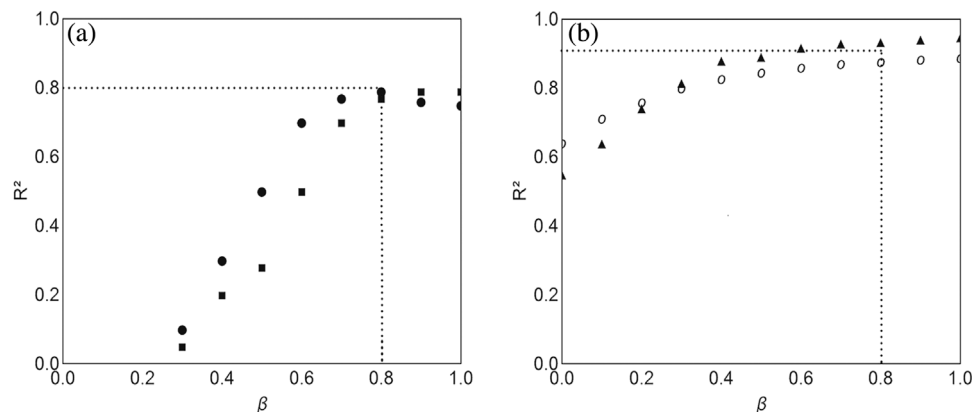


FIGURE 5 Efficiency of the TPB section (β) as a function of the coefficient of adjustment (R^2). (a) Batches without CO_2 injection and (b) Batches with CO_2 injection. Solid circle: Batch 1; solid square: Batch 2; empty circle: Batch 3, and solid triangle: Batch 4

and self-shading, photosynthesis and algal production occurred in these compartments. Through modeling, TPB efficiency was estimated on the basis of its participation in the total productivity of the system. The results of the elaborated adjustments are presented in Figure 5.

Using low values for β , the model expressed saturation before reaching the biomass concentrations obtained experimentally. By considering efficiency very close to 1, the model was made to fit the experimental data, but not with the best possible R^2 . Values of β between 0.80 and 1.00 represented both situations well. We chose $\beta = 0.80$, considering the lower limit. This value was high because it considers the volume in the acrylic tubes directly exposed to irradiance, whereas by considering only the reservoir conditions, the value of β would probably be lower.

3.4 | Temperature data used for model simulation

Temperature data used for modeling were obtained from Hodaifa et al. (2010) who studied the effect of temperature changes on the growth of *S. obliquus* for a wastewater treatment process. The authors determined the upper (T_{max}) and lower (T_{min}) limits to be 37.85 and 0.75°C, respectively. The optimum temperature (T_{opt}) was determined from the maximum growth rate at 29.55°C, close to that obtained by Grobbelaar, Soeder, and Stengel (1990) and, later, Martínez et al. (1999).

3.5 | Adjustment of the model to the experimental data

Table 2 shows the initial and final concentrations of biomass and phosphorus for each batch, and the model adjusted to the experimental data is presented in Figure 6.

The model was able to satisfactorily represent biomass experimental data for all cases ($R^2 > 0.73$) where data with CO_2 injection were better represented. The model was not able to represent phosphorus data satisfactorily in any of the cases. This could have been caused by the fact that P is not directly related to the increase in biomass, which, in turn, can be explained by the luxuriant consumption of phosphorus, being accumulated intracellularly in the form of polyphosphate, a

common condition in green algae under conditions of nutritional imbalance (Chu et al., 2013; Chu, Chu, Shen, Lam, & Zeng, 2014). Under certain conditions polyphosphate is accumulated for use as an internal resource when the external concentration of phosphorus become limiting or because of a shortage of this nutrient in the extracellular environment (Powell, Shilton, Chisti, & Pratt, 2009). However, this phenomenon could not be predicted by the elaborated model.

The effect of irradiance was evident in the model for all batches. In periods when the irradiance received by the system was zero, the specific growth rate remained constant, making the growth null throughout the period. As the saturation of the model occurs, the perception of nocturnal periods is reduced. Table 3 shows the kinetic constants obtained for model fitting to the experimental data of each batch.

For the determination of the kinetic parameters, the efficiency of the TPB section was set to 0.8 with respect to the TLC section, and the K_c value as 0.000028 g L^{-1} according to Cerco and Cole (1995) which obtained this constant from the Monod model. The parameters μ_{max_S} and k_S were obtained from the model fit to the experimental data.

The value of μ_{max_C} was determined according to Cheah, Show, Chang, Ling, and Juan (2015), which states that about 50% of dry biomass is carbon from CO_2 , that is, for each 1 g of biomass it is necessary to fix 1.83 g CO_2 . Knowing the amount of biomass obtained, it was possible to determine the value of k_C so that this relation could be fulfilled. This value was achieved by the integration of the mass transfer model. On the other hand, for the batches without CO_2

TABLE 2 Initial and final conditions of biomass (X) and phosphorus (P) for each batch

Condition	Without CO_2 injection		With CO_2 injection	
	Batch 1	Batch 2	Batch 3	Batch 4
X_0 [g L^{-1}]	0.0300	0.1500	0.1800	0.1000
X_F [g L^{-1}]	0.1732	0.3700	1.2900	1.3320
$S_0 P$ [g L^{-1}]	0.0174	0.0225	0.0443	0.0260
$S_F P$ [g L^{-1}]	0.0015	0.0010	0.0017	0.0003

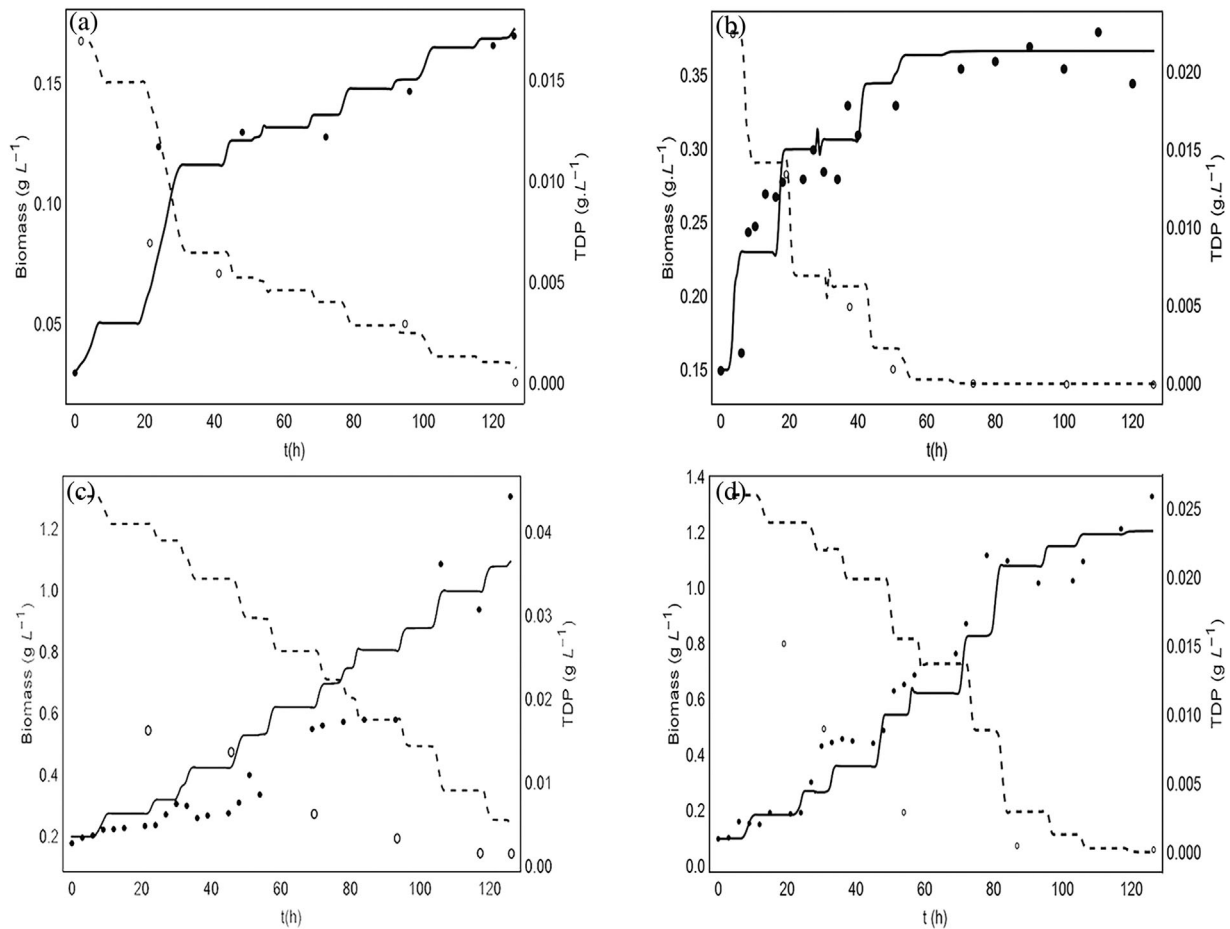


FIGURE 6 Model fitting to the experimental data. (a) Batch 1, (b) Batch 2, (c) Batch 3, and (d) Batch 4. Solid circle, biomass; empty circle, phosphorus; solid line, model fitting representing biomass increase; dotted line, model fitting representing consumption of phosphorus. TDP, total dissolved phosphorus

injection, the value of k_C was increased until all the CO_2 present in the medium was consumed. Values above these were not convenient, since the transfer occurs very slowly.

According to Grobbelaar (2004), the atmospheric CO_2 is insufficient to satisfy the carbon requirements of the high-performance aquatic phototrophic production systems. This is because in phototrophic growth conditions only 5% of the carbon required by the cultures is transferred directly from the atmosphere, which limits growth and consequently lipid production, for example (Stephan, Shockey, Moe, & Dorn, 2002).

From the integral of the mass transfer model it was found that the amount of atmospheric CO_2 transferred to the system in cultures 1, 2,

3, and 4 were, respectively, 49.41, 69.20, 279.99, and 312.93 g. For the cultures without CO_2 injection, the fixed mass was lower because the CO_2 available was consumed and its equilibrium concentration in the atmosphere is very small, thus, the CO_2 replacement in the environment is not favored, causing a lower productivity. In this case, a system of chicanes could be implemented in the TLC section, which could improve this transfer. For the batch with CO_2 injection, the modeling considered the system saturated during the experimental period, that is, all the CO_2 consumed was immediately replaced. The values presented for the mass of CO_2 transferred from the atmosphere to the culture were approximated from the relation of Cheah et al. (2015), previously presented.

TABLE 3 Kinetic parameters obtained by adjusting the growth model to the experimental data

Batch	Kinetic parameter					R^2	Productivity [$\text{g m}^{-2} \text{dia}^{-1}$]
	μ_{maxS} [hr^{-1}]	μ_{maxC} [hr^{-1}]	k_S [g L^{-1}]	k_C [g L^{-1}]	β		
Batch 1	1.00	10.00	0.0900	0.000028	0.80	0.7704	0.8500
Batch 2	1.00	54.00	0.0290	0.000028	0.80	0.7244	0.7750
Batch 3	0.45	95.00	0.0100	0.000028	0.80	0.8774	8.6667
Batch 4	0.40	114.00	0.0095	0.000028	0.80	0.9352	9.3333

As CO₂ is one of the main limiting factors for primary production, once CO₂ deficiency was detected, the injection generated a clear optimization of the system. Growth was shown to be gradual and continuous, without oscillations and losses, a fundamental requirement for system scale up.

When the model was adjusted to the experimental data of Masojídek et al. (2010), it was verified that this system had a S/V ratio >100 m⁻¹, which is considered high, so the efficiency of this reservoir was considered equal 1. In other words, a very small volume of culture that passes through the reservoir will, in association with a lower retention time, have no significant influence on the total productivity of the system. However, this does not apply to the system herein studied since the efficiency determined for the TPB section, which includes the reservoir, was 0.8. To increase this efficiency, it would be necessary to increase the surface area of the TLC section, which would result in optimization in the system.

The mathematical modeling of the system studied here allowed not only its optimization, but also allowed us to evaluate the various system parameters, as well as guide implementation of the system in different situations. The model allows for making a previous evaluation of the temperature and irradiance patterns of any region of the planet and then testing which microorganism could be most appropriate for a given set of environmental conditions. In other words, the modeling was performed in a way that allows insertion of physiological characteristics of the microorganism intended for use. Therefore, even before assembling the equipment, it is possible to verify whether growth will be suitable, or even estimate the productivity through different seasons, depending on where the system will be located. The model also allows testing of the best geometric dimensions to obtain the highest productivity related to the best ratio between the sections to have the best cost/benefit ratio.

In comparison with others, the present model becomes simpler due to the type of experimental arrangement and the reduced number of input variables. According to Solimeno et al. (2015) in open systems such as TLC, parameters related to photorespiration can be disregarded, because the culture flows in a thin layer and with turbulent regime, reducing the oxygen saturation. The model also takes into account the use of environmental factors oscillating throughout the period, unlike the model proposed by Bernard and Rémond (2012), in addition to the aspects of mass transfer, which are mainly involved in the TLC section.

Finally, the built hybrid system performed very well, especially considering the absence of nutrient replacement in the experiments performed. An optimization of the supply of nutrients could increase the productivity potential of the system. As shown by the modeling, this performance could also be improved with changes in the relative dimensions of the sections, optimizing the productivity in a possible scale up.

4 | CONCLUDING REMARKS

The model presented here was able to predict biomass increase for open-air systems, considering the main variables that influence such

biomass increase, including temperature, irradiance, and substrate. Simultaneous variation of these parameters in the model is interesting mainly because in large-scale crops, it is difficult to maintain all of them as constant variables throughout the productive cycle. Moreover, the input parameters are relatively simple and based on knowledge about the geometry of the system, the local environmental conditions and the microorganism to be used. Aspects regarding the luxuriant phosphorus consumption, however, should be better studied so that it can be adapted to the model.

The use of mathematical modeling proposed here also resulted in an improved understanding of the culture system, its possibilities and its weaknesses, evidencing what could be improved in search of optimization and better use of its potential. The modeling also allows us to evaluate patterns of environmental variables, even before the implementation of the experimental unit and to define the best microorganism to be used for each situation based on estimating productivity. The use of specific differential balances for each section (TPB and TLC) allowed us to highlight the characteristics of each one, as well as define the aspects of atmospheric CO₂ transfer to the culture, preserving the conjugated character of the microalgae production system studied. From these balances, it was possible to determine that the efficiency of the TPB section is approximately 80% of that observed in the TLC section. This value is only representative because of the tubes that are attached to the TPB section, which strongly contributed to microalgal growth. For the system to be more productive, the increasing S/V ratio would also be necessary.

Although a targeted evaluation was not made, nutrient replacement would possibly increase the productivity of the system, which was always run in non-fed batches. In this sense, experiments for model validation are foreseen in future studies with this system that can certainly be improved to obtain greater productivity and an even more comprehensive and realistic model.

ACKNOWLEDGMENTS

This work received financial support from the Ministry of Science, Technology and Innovation of Brazil through the Public Call—Energy Potential of Microalgae for the Production of Biodiesel (process CNPq 407513/2013-2). Deise Parolo Tramontin and Pablo Diego Gressler received MSc and PhD scholarship, respectively, from the Coordination for the Improvement of Higher Education Personnel (CAPES). We also thank the support of the Graduate Programs in Chemical Engineering (Pos-ENQ) and Biotechnology and Biosciences (PPG-BB) of the Federal University of Santa Catarina (UFSC).

ORCID

Deise P. Tramontin  <http://orcid.org/0000-0001-9009-4458>

REFERENCES

APHA. (2012). *Standard methods for the examination of water and wastewater*. Washington, DC: American Public Health Association.

- Arar, E. J., & Collins, G. B. (1997). *In vitro determination of chlorophyll-a and pheophytin-a in marine and freshwater algae by fluorescence*. EPA Method 445.0. U.S. Washington, DC: Environmental Protection Agency.
- Béchet, Q., Shilton, A., & Guieysse, B. (2013). Modeling the effects of light and temperature on algae growth: State of the art and critical assessment for productivity prediction during outdoor cultivation. *Biotechnology Advances*, 31, 1648–1663.
- Bernard, O., & Rémond, B. (2012). Validation of a simple model accounting for light and temperature effect on microalgal growth. *Bioresource Technology*, 123, 520–552.
- Bernard, O., Mairet, F., & Chachuat, B. (2015). Modelling of microalgae culture systems with applications to control and optimization. *Advances in Biochemical Engineering/Biotechnology*, 153, 58–87.
- Borowitzka, M. A. (1999). Commercial production of microalgae: Ponds, tanks, tubes and fermenters. *Journal of Biotechnology*, 70, 313–321.
- Cerco, C. F., & Cole, T. (1995). *User's Guide to the CE-QUAL-ICM: Three-dimensional eutrophication model*. Technical Report EL-95-1 5. Vicksburg, MS: U. S. Army Corps of Engineers (p. 320).
- Cheah, W. Y., Show, P. L., Chang, J. S., Ling, T. C., & Juan, J. C. (2015). Biosequestration of atmospheric CO₂ and flue gas-containing CO₂ by microalgae. *Bioresource Technology*, 184, 190–201.
- Chisti, Y. (2013). Constraints to commercialization of algal fuels. *Journal of Biotechnology*, 167, 201–214.
- Chisti, Y. (2016). Large-scale production of algal biomass: Raceway ponds. In: F. Bux and Y. Chisti (Eds.), *Algae Biotechnology. Green Energy and Technology* (pp. 21–40). Springer: Cham.
- Chu, F., Chu, P., Cai, P., Li, W., Lam, P. K. S., & Zeng, R. J. (2013). Phosphorus plays an important role in enhancing biodiesel productivity of *Chlorella vulgaris* under nitrogen deficiency. *Bioresource Technology*, 134, 341–346.
- Chu, F., Chu, P., Shen, X., Lam, P. K. S., & Zeng, R. J. (2014). Effect of phosphorus on biodiesel production from *Scenedesmus obliquus* under nitrogen-deficiency stress. *Bioresource Technology*, 152, 241–246.
- Di Toro, D. M., O'Connor, D. J., & Thomann, R. V. (1971). Dynamic model of the phytoplankton population in the Sacramento–San Joaquin Delta. In R. F. Gould (Ed.), *Nonequilibrium systems in natural water chemistry* (pp. 131–180). Washington: American Chemical Society.
- Doucha, J., & Lívanský, K. (2006). Productivity, CO₂/O₂ exchange and hydraulics in outdoor open high density microalgal (*Chlorella* sp.) photobioreactors operated in a Middle and Southern European climate. *Journal of Applied Phycology*, 18, 811–826.
- Fernández, F. G. A., Camacho, F. G., Pérez, J. A. S., Sevilla, J. M. F., & Grima, E. M. (1998). Modeling of biomass productivity in tubular photobioreactors for microalgal cultures: Effects of dilution rate, tube diameter, and solar irradiance. *Biotechnology and Bioengineering*, 58, 605–616.
- Forget, M. H., Sathyendranath, S., Platt, T., Pommier, J., Vis, C., Kyewalyanga, M. S., & Hudon, C. (2007). Extraction of photosynthesis-irradiance parameters from phytoplankton production data: Demonstration in various aquatic systems. *Journal of Plankton Research*, 29, 249–262.
- Gómez-Villa, H., Voltolina, D., Nieves, M., & Pinã, P. (2005). Biomass production and nutrient budget in outdoor cultures of *Scenedesmus obliquus* (chlorophyceae) in artificial wastewater, under the winter and summer conditions of Mazatlán, Sinaloa, Mexico. *Viet et Mileu*, 55, 121–126.
- Grima, M. E., Fernández, J., Acien, F. G., & Chisti, Y. (2001). Tubular photobioreactor design for algal cultures. *Journal of Biotechnology*, 92, 113–131.
- Gris, B., Morosinotto, T., Giacometti, G. M., Bertucco, A., & Sforza, E. (2014). Cultivation of *Scenedesmus obliquus* in photobioreactors: Effects of light intensities and light-dark cycles on growth, productivity, and biochemical composition. *Applied Biochemistry and Biotechnology*, 172, 2377–2389.
- Grobbelaar, J. U. (2004). Algal nutrition—Mineral nutrition. In A. Richmond (Ed.), *Handbook of microalgal culture—Biotechnology and applied phycology* (pp. 97–115). Oxford: Blackwell.
- Grobbelaar, J. U., Soeder, C. J., & Stengel, E. (1990). Modeling algal productivity in large outdoor cultures and waste treatment systems. *Biomass*, 21, 297–314.
- Guihéneuf, F., Khan, A., & Tran, L. S. P. (2016). Genetic engineering: A promising tool to engender physiological, biochemical, and molecular stress resilience in green microalgae. *Frontiers in Plant Science*, 7, 1–8.
- Guterman, H., Vonshak, A., & Ben-Yaakov, S. (1990). A macromodel for outdoor algal mass production. *Biotechnology and Bioengineering*, 35, 809–819.
- Hariskos, I., & Posten, C. (2014). Biorefinery of microalgae—opportunities and constraints for different production scenarios. *Biotechnology Journal*, 6, 739–752.
- Henkanatte-Gedera, S. M., Selvaratnam, T., Caskan, N., Nirmalakhandan, N., Van Voorhies, W., & Lammers, P. J. (2015). Algal-based, single-step treatment of urban wastewaters. *Bioresource Technol*, 189, 273–278.
- Hiss, H. (2001). Cinética de processos fermentativos. In W. Schmidell, U. A. Lima, E. Aquarone, & W. Borzani (Eds.), *Biotechnologia industrial* (pp. 93–122). São Paulo: Edgard Blücher Ltda.
- Hodaifa, G., Martínez, M. E., & Sánchez, S. (2010). Influence of temperature on growth of *Scenedesmus obliquus* in diluted olive mill wastewater as culture medium. *Engineering in Life Sciences*, 10, 257–264.
- Huesemann, M. H., Wagenen, J. V., Miller, T., Chavis, A., Hobbs, S., & Crowe, B. (2013). A screening model to predict microalgae biomass growth in photobioreactors and raceway ponds. *Biotechnology and Bioengineering*, 110, 1583–1594.
- Idaho Sustainable Energy. (2013). Hybrid algae production system (HAPS) to advance timetable for commercial production.
- Kang, J., & Wen, Z. (2015). Use of microalgae for mitigating ammonia and CO₂ emissions from animal production operations—Evaluation of gas removal efficiency and algal biomass composition. *Algal Research*, 11, 204–210.
- Kaplan, R. S., Pratt, R., & Pedersen, P. L. (1986). Purification and characterization of the reconstitutively active phosphate transporter from rat liver mitochondria. *The Journal of Biological Chemistry*, 261, 12767–12773.
- Kose, A., & Oncel, S. S. (2017). Algae as a promising resource for biofuel industry: Facts and challenges. *International Journal of Energy Research*, 7, 924–951.
- Kumar, K. S., Dahms, H. U., Won, E. J., Lee, J. S., & Shin, K. H. (2015). Microalgae—A promising tool for heavy metal remediation. *Ecotoxicology and Environmental Safety*, 113, 329–352.
- Lee, E., Jalalizadeh, M., & Zhang, Q. (2015). Growth kinetic models for microalgae cultivation: A review. *Algal Research*, 12, 497–512.
- Lívanský, K., & Doucha, J. (1996). CO₂ and O₂ gas exchange in outdoor thin-layer high density microalgal cultures. *Journal of Applied Phycology*, 8, 353–358.
- Lobry, J. R., Rosso, L., & Flandrois, J. P. (1991). A FORTRAN subroutine for the determination of parameter confidence limits in Non-linear models. *Binary*, 3, 86–93.
- Macedo, M. F., Ferreira, J. G., & Duarte, P. (1998). Dynamic behaviour of photosynthesis-irradiance curves determined from oxygen production during variable incubation periods. *Marine Ecology Progress Series*, 165, 31–43.
- Martínez, M. E., Jimenez, J. M., & Yousfi, F. E. (1999). Influence of phosphorus concentration and temperature on growth and phosphorus uptake by the microalga *Scenedesmus obliquus*. *Bioresource Technology*, 67, 233–240.
- Masojidek, J., & Prasil, O. (2010). The development of microalgal biotechnology in the Czech Republic. *Journal of Industrial Microbiology & Biotechnology*, 37, 1307–1317.
- Masojidek, J., Kopecký, J., Giannelli, L., & Torzillo, G. (2010). Productivity correlated to photobiochemical performance of *Chlorella* mass cultures grown outdoors in thin-layer cascades. *Journal of Industrial Microbiology & Biotechnology*, v, 1–11.

- Minhas, A. K., Hodgson, P., Barrow, C. J., & Adholeya, A. (2016). A review on the assessment of stress conditions for simultaneous production of microalgal lipids and carotenoids. *Frontiers in Microbiology*, *7*, 1–19.
- Morales-Amaral, M. M., Gómes Serrano, C., Acién, F. G., Fernández-Sevilla, J. M., & Molina Grima, E. (2015). Outdoor production of *Scenedesmus* sp. in thin-layer and raceway reactors using centrate from anaerobic digestion as the sole nutrient source. *Algal Research*, *12*, 99–108.
- Öncel, S. S., & Akpolat, O. (2006). An integrated photobioreactor system for the production of *Spirulina platensis*. *Biotechnology*, *5*, 365–372.
- Powell, N., Shilton, A., Chisti, Y., & Pratt, S. (2009). Towards a luxury uptake process via microalgae—Defining the polyphosphate dynamics. *Water Research*, *43*, 4207–4213.
- Provasoli, L. (1968). Media and prospects for the cultivation of marine algae. In A. A. Watanabe & A. Hattori (Eds.), *Cultures and collections of algae* (pp. 63–75). Proceedings of the U.S. Japan Conference Hakone, Japanese Society of Plant Physiology, Hakone.
- Pulz, O. (2001). Photobioreactors: Production systems for phototrophic microorganisms. *Applied Microbiology and Biotechnology*, *57*, 287–293.
- Pulz, O., & Scheibenbogen, K. (1998). Photobioreactors: Design and performance with respect to light energy input Advances. In: T Scheper (Ed.), *Biochemical engineering biotechnology* (Vol. 59, pp. 123–152). Berlin: Springer-Verlag.
- Pushparaj, B., Pelosi, E., Tredici, M. R., Pinzani, E., & Materassi, R. (1997). An integrated culture system for outdoor production of microalgae and cyanobacteria. *Journal of Applied Phycology*, *9*, 113–119.
- Quinn, J., Winter, L., & Bradley, T. (2011). Microalgae bulk growth model with application to industrial scale systems. *Bioresource Technology*, *102*, 5083–5092.
- Ritchie, R. J. (2008). Fitting light saturation curves measured using modulated fluorometry. *Photosynthesis Research*, *96*, 201–215.
- Ruiz Marín, A., Mendoza-Espinosa, L. G., & Stephenson, T. (2010). Growth and nutrient removal in free and immobilized green algae in batch and semi-continuous cultures treating real wastewater. *Bioresource Technology*, *101*, 58–64.
- Sevilla, J. M. F., García, M. C. C., Mirón, A. S., Belarbi El, H., Camacho, F. G., & Grima, E. M. (2004). Pilot-plant-scale outdoor mixotrophic cultures of *Phaeodactylum tricornutum* using glycerol in vertical bubble column and airlift photobioreactors: Studies in fed-batch mode. *Biotechnology Progress*, *20*, 728–736.
- Shelp, B. J., & Canvin, D. T. (1980). Photorespiration and oxygen inhibition of photosynthesis in *Chlorella pyrenoidosa*. *Plant Physiology*, *65*, 780–784.
- Solimeno, A., Samsó, R., Uggetti, E., Sialve, B., Steyer, J., Gabarró, A., & García, J. (2015). New mechanistic model to simulate microalgae growth. *Algal Research*, *12*, 350–358.
- Spolaore, P., Joannis-Cassan, C., Duran, E., & Isambert, A. (2006). Commercial applications of microalgae. *Journal of Bioscience and Bioengineering*, *101*, 87–96.
- Steele, J. H. (1962). Environmental control of photosynthesis in the sea. *Limnology and Oceanography*, *7*, 137–150.
- Stephan, D. J., Shockey, R. E., Moe, T. A., & Dorn, R. (2002). *Carbon dioxide sequestering using microalgal systems*. Pittsburgh, PA: U. S. Department of Energy.
- Vega, B. O. A., & Voltolina, D. (2007). Determinación de peso seco y contenido orgánico e inorgánico. In B. O. A. Vega & D. Voltolina (Eds.), *Métodos y herramientas analíticas en la evaluación de la biomasa microalgal* (pp. 27–30). La Paz: CIBNOR.
- Welty, J. R., Wicks, C. E., Wilson, R. E., & Rorrer, G. R. (2008). *Fundamentals of momentum, heat and mass transfer*. New York: John Wiley (p. 803).
- Wilke, C. R., & Chang, P. (1955). Correlation of diffusion coefficients in dilute solutions. *AIChE Journal*, *1*, 264–270.
- Xu, L., Weathers, P. J., Xiong, X. R., & Liu, C. Z. (2009). Microalgal bioreactors: Challenges and opportunities. *Engineering in Life Sciences*, *9*, 178–189.

How to cite this article: Tramontin DP, Gressler PD, Rörig LR, et al. Growth modeling of the green microalga *Scenedesmus obliquus* in a hybrid photobioreactor as a practical tool to understand both physical and biochemical phenomena in play during algae cultivation. *Biotechnology and Bioengineering*. 2017;1–13.
<https://doi.org/10.1002/bit.26510>